AIP The Journal of Chemical Physics

AdeperturbationanalysisoftheB3Σu−(v′=0–6)andth B″3Πu(v′=2–12) states of S2

M. E. Green and C. M. Western

Citation: J. Chem. Phys. **104**, 848 (1996); doi: 10.1063/1.470810
View online: http://dx.doi.org/10.1063/1.470810
View Table of Contents: http://jcp.aip.org/resource/1/JCPSA6/v104/i3
Published by the American Institute of Physics.

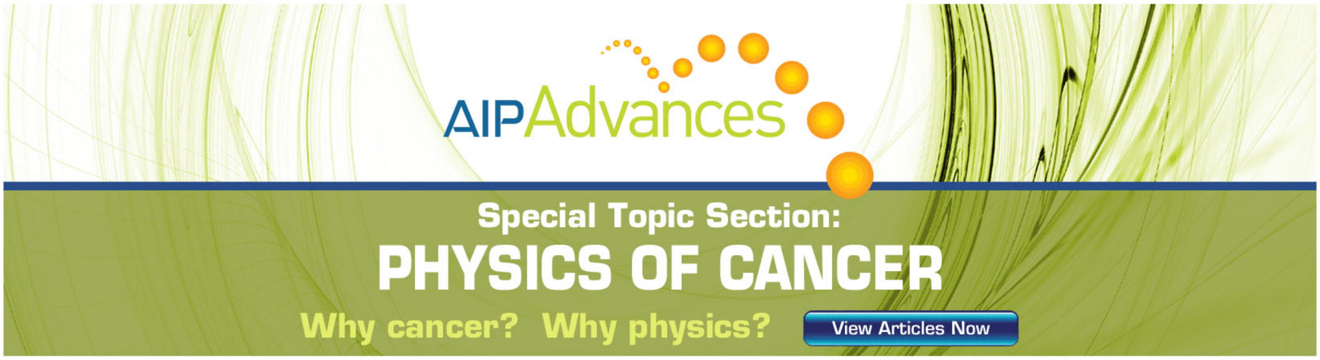

A deperturbation analysis of the $B\ ^3\Sigma_u^-(v'=0-6)$ and the $B''\ ^3\Pi_u(v'=2-12)$ states of S_2

M. E. Green and C. M. Western
School of Chemistry, University of Bristol, Cantock's Close, Bristol BS8 1TS, United Kingdom

(Received 1 August 1995; accepted 10 October 1995)

Laser-induced fluorescence spectra of $^{32}S_2$ have been obtained, covering $v'=0-6$ of the $B\ ^3\Sigma_u^- - X\ ^3\Sigma_g^-$ transition and $v'=2-12$ of the $B''\ ^3\Pi_u - X\ ^3\Sigma_g^-$ transition, using static cell and supersonic free jet techniques. The spectra include transitions to the previously unseen $B''\ ^3\Pi_{2,u}$ components. Analysis of the many perturbations between the two upper electronic states has been carried out using a Hamiltonian matrix including all the B and B'' states simultaneously rather than deperturbing individual pairs of vibronic states. This takes into account longer range interactions and gives deperturbed molecular constants that vary smoothly with vibrational state. Our model for the B'' $v'=2-12$ and B $v'=0-6$ levels covering J up to 100 can fit all 3320 observed transitions with an average error of 0.064 cm^{-1}. The widely ranging fluorescence lifetimes of the B'' state vibronic levels provide independent information about the state mixing and confirm the model, since the observed $B''-X$ fluorescence arises almost entirely via this mixing. However, lifetime measurements of the newly observed $\Omega=2$ components of the B'' state showed little variation in lifetimes, about an average of $4.2\pm0.4\ \mu$s. This indicates a small intrinsic $B''-X$ transition strength as the $\Omega=2$ components are essentially not mixed with the B state. A model for the perturbation parameters is developed, based on Franck–Condon factors between the two states. The magnitude of the perturbations and transition moments are discussed in relation to the electronic configurations of the B and B'' states. © *1996 American Institute of Physics.* [S0021-9606(96)01303-5]

I. INTRODUCTION

The $B\ ^3\Sigma_u^- - X\ ^3\Sigma_g^-$ transition of S_2 in the ultraviolet is a strong transition which should be ideal for laser-induced fluorescence (LIF) probing of S_2. However, despite the fact that this transition has been studied for over 80 years,[1] a full rotational analysis has never been carried out. This is hindering work on dynamical studies involving the measurement of internal state distributions of S_2 as a reaction product, as mentioned in investigations into the photodissociation of CS_2 (Ref. 2) and the reaction of OCS with $S(^1D)$ atoms.[3] The recent observation of this transition by the Hubble Space Telescope in the perturbed stratosphere of Jupiter after the collision of the comet Shoemaker–Levy 9,[4] has also illustrated the need for an accurate model of the S_2 absorption bands. The problem with the analysis lies with the extensive perturbations in the system which are now known to be due to a single state, the $B''\ ^3\Pi_u$. The potential energy curves of the B and B'' states are given in Fig. 1, where the two states can be seen to overlap over a wide range of vibrational levels. The interaction between the B and B'' states is analyzed in detail in this paper and provides a model for understanding highly perturbed systems. It also provides some interesting insights into the electronic configurations of the states involved, which turn out to be not entirely straightforward. The traditional molecular configurations of the three states involved are given below

$$B\ ^3\Sigma_u^- \quad \cdots 5\sigma_g^2 2\pi_u^3 2\pi_g^3,$$

$$B''\ ^3\Pi_u \quad \cdots 5\sigma_g^2 2\pi_u^4 2\pi_g^1 5\sigma_u^1\ ,$$

$$X\ ^3\Sigma_g^- \quad \cdots 5\sigma_g^2 2\pi_u^4 2\pi_g^2.$$

The $B-X$ absorption bands in S_2 are analogous to the extensively studied Schumann–Runge bands in O_2. The transition may be readily observed as a strong absorption in S_2 vapor, and appears as a long progression of bands. The coarse vibrational structure of these bands is fairly straightforward with the bands becoming diffuse above $v'=9$, due to their being above the dissociation limit as shown in Fig. 1, and therefore predissociated.[5] The rotational analysis of these bands, however, has proved to be far from trivial. Early work, as summarized by Barrow and du Parcq[6] mainly consisted of partial rotational analyses of relatively unperturbed regions of the system. Investigations into the perturbed nature of the system were first carried out by Meakin and Barrow,[7] who found many rotational perturbations in the vibrational levels $v'=7$ and 8, and suggested that they were due to a perturbing state of $^3\Pi_u$ symmetry, now labeled B''. Further investigations by Meyer and Crosley[8] illustrated the erratic behavior of some of the B state molecular constants due to the extensive perturbations in the system. For example they found that the spin–spin splitting constant λ of the B state, which would normally vary smoothly with vibrational state, behaved anomalously having values of $\lambda\approx-4.7\ \mathrm{cm}^{-1}$ for $v'=0,2,4$ and $\lambda\approx+9.5\ \mathrm{cm}^{-1}$ for $v'=1,3,5$. This alternation gives a quite different appearance to vibrational bands with odd and even v as the satellite branches such as $^TR_{31}$ having significant intensity where λ has the opposite sign to the ground state.

Although spin and orbitally allowed, the $B''-X$ transitions are much weaker than the $B-X$ transitions and were not seen directly for many years. Bondybey and English[9] were the first to directly observe $B''-X$ transitions in their

0021-9606/96/104(3)/848/17/$6.00

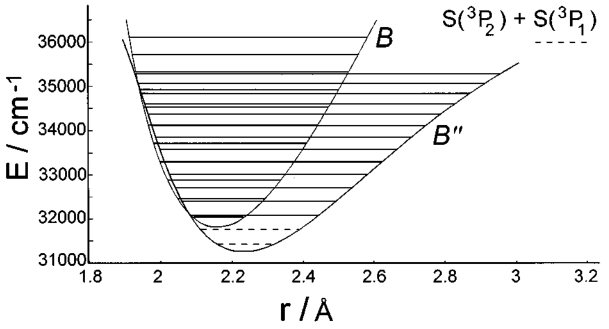

FIG. 1. RKR potential energy curves of the B and B'' states of S_2. Vibrational levels in the B state above $v'=9$ are above the dissociation limit and hence predissociated. The solid lines represent observed levels whereas the dashed lines represent levels extrapolated from the measured data.

study of S_2 isolated in rare gas matrices. By studying fluorescence emission and excitation spectra, they reassigned fluorescence that had previously been attributed to transitions from the B state as being from the B'' state and tabulated a vibrational progression of this state for $v'=0$–6. Quick and Weston[10] measured fluorescence lifetimes for S_2 vapor excited to the B state and observed additional low intensity peaks with increased lifetimes and attributed these to perturbations by the B'' state. The first deperturbation analysis of the $B-X$ system was carried out by Patiño and Barrow[11] for the $v'=1$ levels of the B state. They derived constants for the perturbing state confirming that it was $^3\Pi_u$ and, by measuring isotopic shifts of the deperturbed levels, they estimated T_e for the B'' state to be 31 070 cm^{-1}, which was found to be consistent with the matrix work.[9] A deperturbation analysis was also carried out by Heaven *et al.*[12] on the $B\ v'=2$ state for $J\leqslant30$, again obtaining constants for the perturbing state. They used supersonic free jet methods to produce molecules with low rotational temperatures, leading to less congested spectra.

As a consequence of the $B''-X$ transitions being much weaker than the $B-X$ transitions, the radiative lifetimes of the B'' states are longer than for the B states. By combining supersonic free jet methods with lifetime separation methods Matsumi *et al.*[13] produced greatly simplified LIF spectra, which enabled the weak $B''-X$ transitions to be seen. By setting a time gate across the fluorescence decay curve to measure the fluorescence produced a certain time after the laser had fired, fluorescence from a B'' state could be selectively measured, while discriminating against B state fluorescence. From the spectra of the $B''-X$ bands, rotational constants and term values for the $B''\Omega=0$ and 1 states were obtained for $v'=3$–18. A time-resolved study of the B and B'' states was also carried out by Matsumi *et al.*[14] where fluorescence decay rates were measured for individual rovibronic levels of the two electronic states. They found that the fluorescence lifetimes depended strongly on v and Ω but not J. The measured values for the $B\ ^3\Sigma_u^-$ state varied between 34.2 and 49.3 ns whereas those of the $B''\ ^3\Pi_u$ states varied to a much greater extent, between 106 and 3888 ns. This variation of lifetimes was interpreted in terms of the homogeneous interactions between the B and the B'' states, and interaction strengths between the two states were evaluated. It was assumed throughout these calculations that the intrinsic transition moment for the $B''-X$ transition is negligibly small and therefore that the $B''-X$ transitions are only observed due to the borrowing of transition moment from the $B-X$ transition.

In this paper we describe rotationally cold LIF spectra of $B''-X$ and $B-X$ bands of S_2 produced in a supersonic free jet and rotationally hot $B-X$ spectra from S_2 produced by photolysis. In analyzing the spectra we also use the results of earlier work by Barrow and co-workers[15,16] who obtained absorption (plate) spectra of sulfur vapor at 1025 K using a Jarrell–Ash 3.4 m Ebert spectrograph. The range of J covered in this work is therefore extensive with low J term values for both $B''-X$ and $B-X$ transitions being obtained from the molecular beam spectra, and high J information on the B state being provided by both the room temperature photolysis work and the higher temperature work of Barrow and co-workers. A particular feature of this work is the observation of the formerly unseen $\Omega=2$ bands which has led to a more complete picture of the system, including the determination of the B'' spin–spin constants and hence the modification of the band origins and spin–orbit constants. The measurement of the fluorescence lifetimes of these $\Omega=2$ states also indicates some intrinsic transition moment for the $B''-X$ transition which was previously assumed to be negligible.

The above data are deperturbed to provide a model for the position and intensity of all the observed transitions. Although in previous work individual states have been deperturbed,[11,12] the states involved were treated as though they existed in isolation, so that interactions with more distant states where there are no avoided crossings were not included in the calculations. As there are large homogeneous (J independent) interactions which can mix distant states, this type of deperturbation is incomplete and yields only effective molecular constants which often vary erratically with vibrational state and/or parity. An example of this is found in the work of Patiño and Barrow[11] referred to above; they had to fit e and f parity components separately to give a good fit. It is clear from the analysis performed here that many B'' states interact with more than one B state, and so the deperturbation must be extended to include these long-ranging interactions. The ideal deperturbation procedure is to fit the experimental data for as many states as possible in a simultaneous variation of all the parameters in an appropriate combined Hamiltonian matrix. Here we describe such a deperturbation of the vibrational levels of the B state from $v'=0$ to 6 and of the B'' state from $v'=2$ to 12. The density of states increases rapidly above this level, and so the higher levels $v'=7$–9 of the B state and $v'=13$–18 of the B'' state will be analyzed in a separate fit and form the basis of a separate publication.

II. EXPERIMENT

Information on the $B-X$ transitions came from three sources. LIF spectra at ~300 K were obtained from S_2 generated by a photoinitiated reaction of H_2S in a static cell. A 25% mixture of H_2S in argon at a pressure of $\sim$10 Torr was photodissociated by 266 nm light from a Nd:YAG (Spectron Laser Systems SL802) to produce S_2, most probably via the radical–radical reaction mechanism described by Heaven *et al.*[12] The S_2 produced was then probed by the frequency doubled output of a dye laser (Spectra Physics PDL3) pumped by a Nd:YAG (Quanta-Ray GCR 18S). The spectral width of the UV light was approximately 0.1 cm^{-1} and its power was adjusted to avoid gross saturation. A delay of $\sim$10 μs between the photolysis beam and the pump beam was needed to allow time for secondary photochemical reactions to occur and produce S_2. By varying this delay, the degree of collisional cooling and hence the rotational temperature could be controlled to some extent. The fluorescence produced was collected at 90° to the laser beams and detected with a photomultiplier (Thorn EMI 9125QB). The signal from the photomultiplier was sent directly to a Lecroy (9400A) digital oscilloscope where a gate was set across the fluorescence decay curve. The time gate was set to start collecting signal $\sim$10 ns after the laser had fired to minimize scattered light and had a width of $\sim$50 ns. The spectra obtained in this way gave information on the rotational levels of the B state up to $J\approx50$. The congested nature of the spectra often resulted in the overlap of vibrational bands making assignment difficult. In these cases a monochromator was placed before the photomultiplier which allowed discrimination between transitions to different lower vibrational states, thereby allowing individual vibrational bands to be observed. Information on the $B-X$ transition also came from static cell absorption spectra of S_2 at temperatures over 1000 K, taken by Barrow and co-workers[15,16] some years before. These rotationally hot spectra provided term values for levels with J up to 100, allowing many high J avoided crossings to be observed. The lowest J levels, which could not be obtained from the static cell spectra due to the high level of congestion around the bandheads, were taken instead from the less congested molecular beam spectra.

Rotationally cold laser-induced fluorescence spectra of both the $B-X$ and $B''-X$ transitions were obtained using supersonic free jet methods. A mixture of H_2S in argon ($\sim$1%) was passed through a pulsed electric discharge nozzle and then through a 1 mm pinhole to a region of low pressure (10^{-4} Torr). The pulsed electric discharge nozzle has been described in detail by Western *et al.*,[17] but basically consists of a plastic (Delrin) piece with a $\sim$1-mm-diam, 1-cm-long channel for the gas, mounted on a pulsed molecular beam valve. The electric discharge is provided by a pair of tungsten electrodes mounted halfway down the channel, across which a voltage ($<$1 kV) is applied as the gas is passed through. The pressure behind the nozzle was variable in the range of 0–40 psi and this gave some control over the rotational temperature in the supersonic free jet. A probe beam, produced as before, crossed the molecular beam $\sim$10 mm downstream from the nozzle and the fluorescence was collected at 90° to both the molecular beam and laser beam. The signal was again collected by a photomultiplier, and sent directly to the digital oscilloscope, where various time gates were set across the fluorescence decay curve, allowing the fluorescence produced at different times to be sampled. In this way discrimination could be obtained between the short lived ($\sim$30 ns) fluorescence from the B state and the longer lived ($>$100 ns) fluorescence from the B'' states.

Wavelength calibration for both supersonic free jet and the static cell experiments was obtained by simultaneously recording the laser-induced fluorescence spectrum of iodine vapor (using undoubled light from the dye laser) and interference fringes from a 1 cm^{-1} free spectral range etalon. The line positions were taken directly from the spectra by using a center of mass algorithm on the digitally recorded data. This allowed line positions to be determined to better than the experimental linewidth of $\sim$0.1 cm^{-1}. The iodine calibration spectra were typically fitted to 0.01 cm^{-1} in the visible, leading to a measurement accuracy of 0.02 cm^{-1} in the ultraviolet for strong, unblended lines.

In order to measure the fluorescence lifetimes, the laser was tuned to the frequency of a single low J transition and the fluorescence collected as before. The output of the photomultiplier was sent to the digital oscilloscope where the fluorescence decay profile was averaged over 100–2000 shots. For each lifetime measurement, a recording of the background light was obtained by recording the same number of shots of the output from the photomultiplier with the laser slightly detuned from the transition of interest. This was subtracted from the fluorescence decay profile, leaving a resultant decay curve from which a lifetime value was obtained by least-squares fitting to a single exponential.

III. RESULTS

LIF spectra of $B-X$ bands $v'=0-6$ and $B''-X$ bands $v'=2-12$ were taken. Transitions to the $\Omega=0$ and 1 levels of the B'' state were observed as well as transitions to the very weak and hence previously unobserved $\Omega=2$ levels. The supersonically cooled spectra of the B'' bands had rotational temperatures typically in the range of 5–30 K and hence gave information up to $J\approx20$. The vibrational cooling in the supersonic jet was not as efficient as the rotational cooling, with the result that many of the observed bands were hot bands. This proved advantageous as many of the Franck–Condon factors between low vibrational levels of the ground states and B vibrational states are very low.[18] A typical spectrum showing the $B''-X$ (10–0) and the $B-X$ (7–1) bands with a rotational temperature of 15 K is given in Fig. 2. The upper trace was taken using a time gate set to collect fluorescence produced 200–2000 ns after the laser was fired, and hence shows only the B'' state with a long fluorescence lifetime. The time gate for the lower trace was set to collect fluorescence produced immediately after the scattered light from the laser, and hence shows both the $B''-X$ band and the B state with a much shorter fluorescence lifetime. Although the two bands in the lower trace have similar intensity, this is misleading as the $B-X$ transitions are many times stronger than the $B''-X$ transitions. The apparent similarity in intensity is due both to saturation of the $B-X$ transition, and the

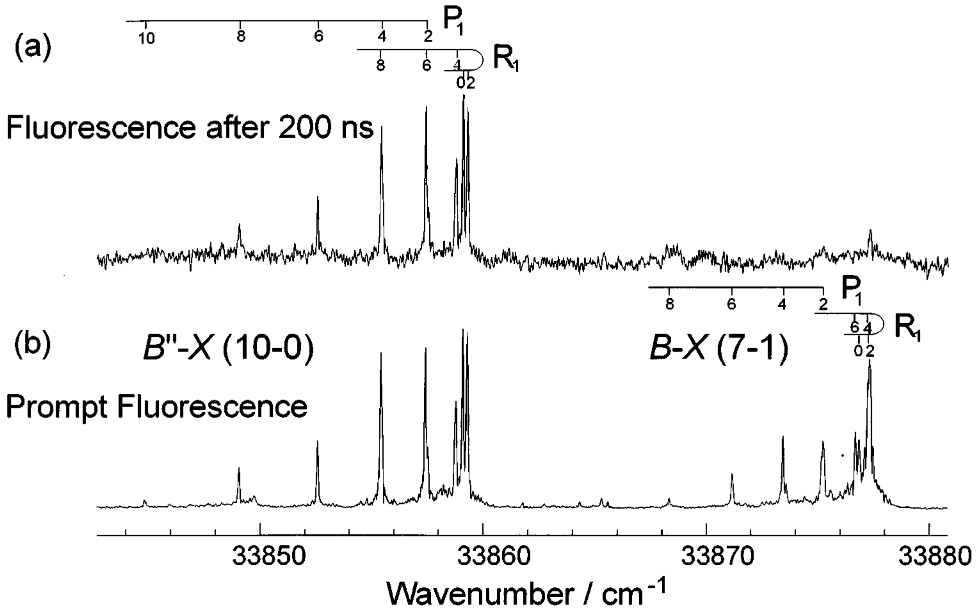

FIG. 2. LIF molecular beam spectra of the $B''-X(10-0)$ and the $B-X(7-1)$ bands; a time gate was set to collect fluorescence produced (a) 200–2000 ns after the laser was fired and (b) immediately after the laser was fired.

fact that the time gate was set to discriminate against scattered light, which therefore cut out much of the B state fluorescence.

Spectra of the mixed isotope $^{34}S\ ^{32}S$ species (8% natural abundance) were not observed in this work. This is perhaps surprising, given the high signal to noise obtained in most spectra (see Figs. 2 and 6). However the $^{34}S\ ^{32}S$ species has twice the number of rotational lines as $^{32}S_2$ because of the nuclear spin statistics. (The symmetric isotope has alternate rotational levels missing.) With our resolution this means that vibronic bands from the mixed isotope will have poorly resolved rotational structure, and will appear as a weak continuous background under the stronger $^{32}S_2$ signals.

Fluorescence lifetimes of B'' bands were measured in the molecular beam and are given in Table I. We found the same wide range of lifetimes (100–1600 ns) as Matsumi *et al.*[14] for the $\Omega=0$ and 1 levels. Measurement of the lifetimes of the $\Omega=2$ levels required particular care; not only were the signals weak because of the weak excitation transitions, but also the fluorescence lifetimes are sufficiently long that molecules can fly out of the viewing region before fluorescing, artificially depressing the apparent fluorescence lifetime. The $\Omega=2$ state transients were therefore recorded with all the normal fluorescence collection optics removed, so there was only a flat window between the photomultiplier and the molecular beam. To check that this arrangement allowed accurate measurement of the fluorescence decay we performed two tests. First we measured lifetimes of the $v=0$ and 1 of the $A\ ^3\Pi_1$ state of SO; these are known to have very long lifetimes[19,20] of 39.2 and 17.1 μs, respectively. Measurements on our apparatus gave lifetimes of 29 and 13.5 μs, though the picture was slightly confused by the observation of strong quantum beats. These figures suggest the require-

TABLE I. Fluorescence lifetimes of the $B''\ ^3\Pi_u$ state of S_2. The figures in parentheses for the data of Matsumi *et al.* are three standard deviations. The estimated errors for the lifetimes measured here are ±10%.

v'	Ω'	τ_f/ns (this work)	τ_f/ns Matsumi *et al.*[c]
2	0	623	
2	1	182	
2	2	4167[a]	
3	1	322	296 (24)
3	2	4375	
4	0	125	155 (42)
4	1	1025	1126 (99)
4	2	b	
5	0	247	204 (21)
5	1	738	717 (93)
5	2	4296	
6	0	773	819 (57)
6	1	118	108 (9)
6	2	4042	
7	0	495	556 (72)
7	1	1039	1057 (99)
7	2	4243	
8	0	167	164 (9)
8	1	887	896 (75)
8	2	4123	
9	0	907	947 (45)
9	1	154	139 (12)
9	2	3982	
10	0	393	393 (36)
10	1	1729	1661(222)
10	2	b	
11	0		338 (21)
11	1		358 (39)
11	2	4076	

[a] Corrected value—see the text.
[b] States with strongly J-dependent lifetimes.
[c] Reference 14.

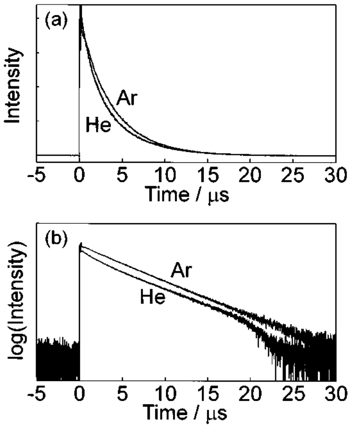

FIG. 3. Fluorescence intensity (a) and the log of the fluorescence intensity (b) plotted against time for a $B''\ ^3\Pi_{2,u}-X\ ^3\Sigma_g^-(9-0)$ transition recorded using both helium and argon mixtures.

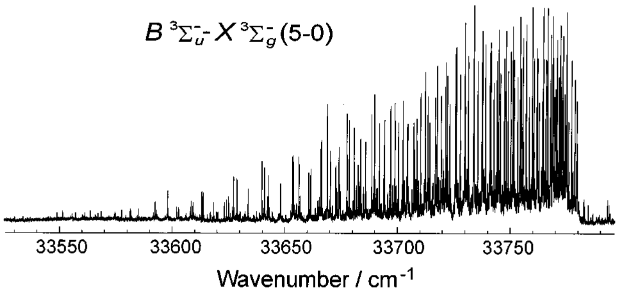

FIG. 5. LIF spectrum of the $B-X(5-0)$ band, produced by the photolysis of H_2S in a static cell.

ment for some corrections to lifetimes much longer than those we observed for any of the B'' states.

Second some B'' $\Omega=2$ lifetimes were recorded using two different carrier gases for the molecular beam, helium, and argon. As the gas mixtures were very dilute this implies a velocity difference of ~3 between the two mixtures, but nevertheless very similar fluorescence decay curves were observed, as shown in Fig. 3. This shows the same transition [from the $B''\ ^3\Pi_{2,u}-X\ ^3\Sigma_g^-$ (9-0) band] recorded using helium and argon mixtures. Note that the helium curve shows nonlinearity in the log plot after 20 μs; this corresponds to a distance of around 3 cm. The lifetimes obtained from these two curves are close, being 3.93 μs (Ar) and 4.16 μs (He). This sort of variation was also typical of repeated measurements taken with the same gas mixture, and probably arises from incomplete subtraction of background light, and problems produced in the photomultiplier by the very strong signals at $t=0$ from strong B state fluorescence. Taking these factors into account we estimate the error on these lifetime measurements to be 0.4 μs. Given this uncertainty the small variation shown in lifetimes for the $\Omega=2$ states in Table I is probably not significant and the most useful number is the average over all the $\Omega=2$ measurements, 4.16 μs.

For B'' $v=2$, $\Omega=2$ the signal was so weak that the lifetime could not be measured without the fluorescence collection optics. The value quoted in Table I was therefore measured with the optics and corrected by comparing measurements for B'' $v=3$ with the same optics. We do not quote lifetimes for B'' $v=4$ and 10 as these showed a very strong variation with J. This is readily understood in terms of the model developed below as both these states undergo a strong, J-dependent mixing at low J with B state levels that are very close in energy.

A spectrum of a $\Omega=2$ band [$B''-X$ (6–3)] is given in Fig. 4(a), taken using a time gate set to collect fluorescence produced 1630–4130 ns after the laser had fired. A simulation of this band is shown in Fig. 4(b) using the model described below.

A typical spectrum of a $B-X$ band of S_2 produced by the photolysis of H_2S in a static cell is shown in Fig. 5. The spectrum was taken using a monochromator in order to discriminate against overlapping bands, and shows the $B-X$ (5–0) band with a rotational temperature of ~300 K. A por-

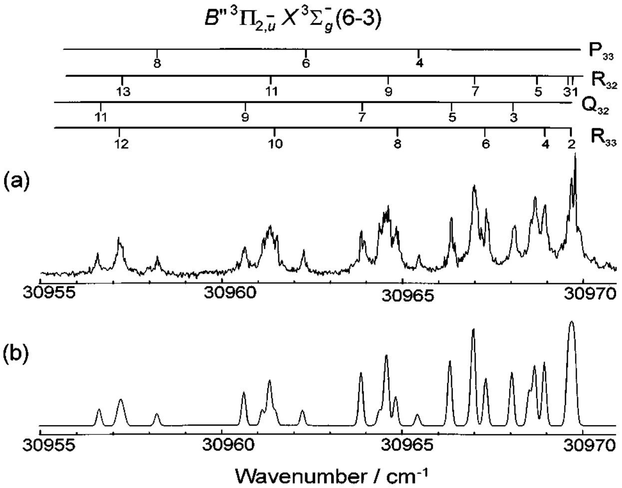

FIG. 4. LIF molecular beam spectrum (a) and simulation (b) of the $B''\ ^3\Pi_{2,u}-X\ ^3\Sigma_g^-(6-3)$ band; the spectrum was taken using a time gate set to collect fluorescence produced 1630–4130 ns after the laser had fired.

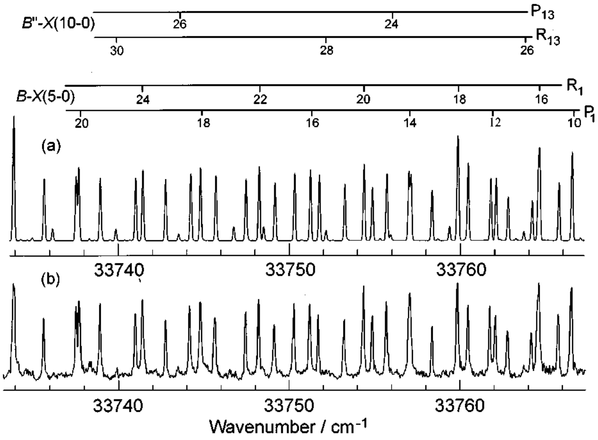

FIG. 6. (a) A simulation and (b) the observed spectrum of part of the $B-X(5-0)$ band shown in Fig. 5. Assignments are shown for some of the branches present in the spectrum; note that some weak transitions from the $B''-X(10-0)$ band also show in this region.

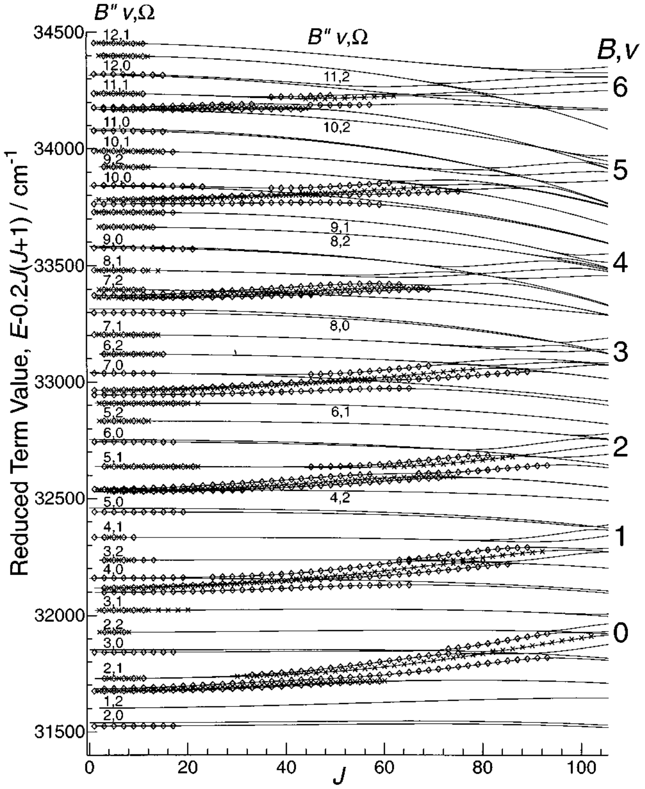

FIG. 7. Observed upper state reduced term [term values $-0.2J(J+1)$] plotted against J for $v'=0$–6 for the B state and $v'=2$–12 for the B''. The ◇ and × are observed term values of e and f parity, respectively, and the solid lines are calculated term values, using the model described in the text. The large numbers on the right-hand side of the diagram indicate the position of the B state vibrational levels. The smaller numbers on the diagram indicate v and Ω for the B'' states; the numbers on the left-hand side refer to the curve immediately below whereas the numbers in the middle refer to the curve immediately above.

tion of this spectrum is shown in Fig. 6 together with a simulation using the model developed below. This shows some weak transitions from the B'' $v'=10$ state, as well as stronger transitions from the B $v'=5$ state.

IV. ANALYSIS

A. Assignment

Rotational analysis and assignment was carried out using the method of combination differences based initially on ground state constants taken from Fourier transform infrared spectra[21] for $v''=0$ and 1 and from emission studies[16] for the other vibrational states. Rotational combination differences were found within each vibrational upper state, and to confirm vibrational assignments, vibrational combination differences were found for each B and B'' vibrational state. The reduced term values, the observed upper state term values minus $0.2J(J+1)$ cm^{-1}, are plotted in Fig. 7 as a function of J for $v'=0$–6 of the B state and $v'=2$–12 of the B'' states. The solid lines in Fig. 7 are term values calculated from the model described below. The ground state term values required to convert the observed transitions to upper state term values were calculated from the refined ground state constants given in Table II, described below.

It is clear from this energy level diagram why analysis of the B state is so difficult; each vibrational level of the B state is perturbed by at least two different vibrational levels of the B'' state. This gives several avoided crossings in the rotational levels of the B state, to a degree that varies dramatically with vibrational state depending on which Ω component crosses the B state and the J value of the crossing. An expanded view of the rotational term values of one B state vibronic level is shown in Fig. 8; note the contrast between the small avoided crossing from the B'' $\Omega=2$ state (shown in the inset), and the much larger crossing with the $\Omega=1$ state.

B. Hamiltonian

The system has been modeled by a computer program PGOPHER, which uses a fairly conventional effective Hamiltonian for a linear molecule. The major terms include the spin–orbit coupling ($A\hat{\mathbf{L}}\cdot\hat{\mathbf{S}}$) and the rotational kinetic energy ($B\hat{\mathbf{R}}^2$);

$$\begin{aligned}\hat{H}&=B(\hat{\mathbf{J}}-\hat{\mathbf{L}}-\hat{\mathbf{S}})^2+A\hat{\mathbf{L}}\cdot\hat{\mathbf{S}}\\&=B[J(J+1)+S(S+1)-\hat{J}_z^2-\hat{L}_z^2-\hat{S}_z^2]+A\hat{L}_z\hat{S}_z\\&\quad-B[(\hat{J}_-\hat{L}_+)+(\hat{J}_+\hat{L}_-)]+(\tfrac{1}{2}A+B)\{\hat{L}_+\hat{S}_-+\hat{L}_-\hat{S}_+\},\end{aligned}\tag{1}$$

where J, L, S, and N have the conventional definitions as given in Lefebvre-Brion and Field.[22] The minor terms are

TABLE II. Refined constants for the $X\ ^3\Sigma_g^-\ v''=0$–5, 7 levels. Figures in parentheses are three standard deviations.

Xv''	$T_{v,0}$ (cm^{-1})	B'' (cm^{-1})	D'' (10^{-7} cm^{-1})	γ'' (cm^{-1})	λ'' (cm^{-1})	λ_D'' (10^5 cm^{-1})
0	0	0.294 592 3 (4)[a]	1.96 (2)[a]	−0.007 157 (9)[a]	11.7931 (4)[a]	1.05(5)[a]
1	719.995(90)	0.292 997 5(23)[a]	1.97 (2)[a]	−0.007 148(28)[a]	11.8659(10)[a]	1.05[a]
2	1434.25(10)	0.291 423 (55)	1.96 (17)	−0.005 93 (91)	11.937 (14)	
3	2142.85(11)	0.289 646 (72)	1.97 (12)	−0.006 6 (14)	12.021 (20)	
4	2845.61(14)	0.288 376 (44)	2.046(62)	−0.007 22 (51)	12.091 (19)	
5	3542.94(52)	0.284 4 (27)	2.12[b]	−0.007 283[b]	12.163[b]	
7	4920.03(22)	0.283 241 (49)	1.987(63)	−0.009 62 (59)	12.247 (25)	

[a] Reference 21.
[b] Reference 16.

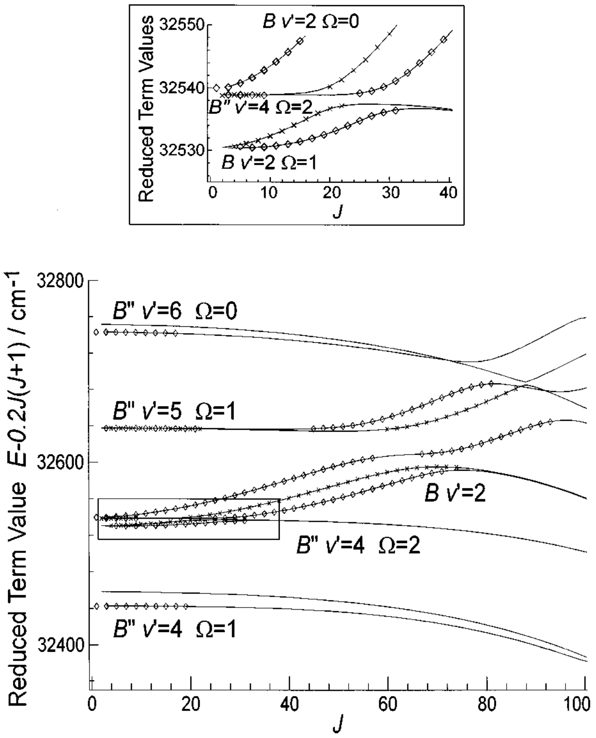

FIG. 8. Expanded view of the observed reduced term values for the B state $v'=2$ and its neighboring B'' states. The inset shows the $B''\ ^3\Pi_{2,u}$ $v'=4$ state crossing the $B\ ^3\Sigma_{1,u}^-$ $v'=2$ state. The ◇ and × are observed term values of e and f parity respectively and the solid lines are calculated term values.

$$\hat{H}' = -D\hat{\mathbf{R}}^4 + \tfrac{2}{3}\lambda(3\hat{S}_z^2-\hat{\mathbf{S}}^2) + \tfrac{1}{2}\lambda_D[\tfrac{2}{3}(3\hat{S}_z^2-\hat{\mathbf{S}}^2),\hat{\mathbf{N}}^2]_+ + \gamma\hat{\mathbf{N}}\cdot\hat{\mathbf{S}} - \tfrac{1}{2}o(\hat{S}_+^2 e^{-2i\phi}+\hat{S}_+^2 e^{+2i\phi}), \tag{2}$$

where $[\hat{O},\hat{Q}]_+ = \hat{O}\hat{Q}+\hat{Q}\hat{O}$. This includes centrifugal distortion (D), spin–spin coupling (λ), and its centrifugal distortion (λ_D), spin–rotation coupling (γ), and the $\Omega=0$ lambda doubling, o. We do not include the terms p and q conventionally used to describe Λ doubling in the Π state; this is discussed further below.

The terms containing $L_\pm$ in Eq. (2) give matrix elements off-diagonal in electronic state and are responsible for the perturbations between the B and B'' states. These matrix elements cannot be evaluated directly and so are taken as parameters in the fit. The spin–orbit parameter (α) and the L-uncoupling parameter (β) are defined as

$$\alpha = \langle B''\Lambda=1|(\tfrac{1}{2}A+B)\hat{L}_+|B\Lambda=0\rangle, \tag{3}$$

$$\beta = \langle B''\Lambda=1|B\hat{L}_+|B\Lambda=0\rangle. \tag{4}$$

Note that these are defined in an unsymmetrized basis. The Hamiltonian matrix is made up in a symmetrized Hund's case (a) basis with the phase of the electronic wave functions defined such that states of ± parity are given by

$$|J\Omega\eta\Lambda S\Sigma^\pm\rangle = \tfrac{1}{\sqrt{2}}\{|J\Omega\eta\Lambda S\Sigma\rangle \pm(-1)^{J-S+s}|J-\Omega\eta-\Lambda S-\Sigma\rangle\}, \tag{5}$$

where s is 1 for a Σ^- state and 0 otherwise. This is consistent with the phase convention of Lefebvre-Brion and Field.[22] Note that this is different from the phase convention used in earlier work on S_2 (Refs. 11 and 14), which used matrix elements taken from Wicke *et al.*[23] In our symmetrized basis the matrix elements off diagonal in the electronic state are

$$\langle ^3\Pi_2|\hat{H}|^3\Sigma_1^-\rangle = -(x-2)^{1/2}\beta, \tag{6}$$

$$\langle ^3\Pi_1|\hat{H}|^3\Sigma_1^-\rangle = 2^{1/2}(\alpha+\beta), \tag{7}$$

$$\langle ^3\Pi_0|\hat{H}|^3\Sigma_1^-\rangle = \mp x^{1/2}\beta, \tag{8}$$

$$\langle ^3\Pi_0|\hat{H}|^3\Sigma_0^-\rangle = (1\pm1)(\alpha+\beta), \tag{9}$$

$$\langle ^3\Pi_1|\hat{H}|^3\Sigma_0^-\rangle = -(1\pm1)(\tfrac{1}{2}x)^{1/2}\beta, \tag{10}$$

where $x=J(J+1)$ and the upper sign corresponds to e parity and the lower sign to f parity.

It was found necessary to include centrifugal distortion of the perturbation parameters to model the high J crossings accurately. The required operators in the Hamiltonian were defined by analogy to the centrifugal distortion of other fine structure constants as defined by Hirota *et al.*:[24]

$$\tfrac{1}{2}\alpha_D'[\hat{\mathbf{R}}^2,L_+S_-+L_-S_+]_+ + \tfrac{1}{2}\beta_D'[\hat{\mathbf{R}}^2,L_+J_-+L_-J_+]_+ . \tag{11}$$

The parameters for these terms are defined by the following matrix elements:

$$\alpha_D = \langle B''\Lambda=1|\alpha_D' L_+|B\Lambda=0\rangle, \tag{12}$$

$$\beta_D = \langle B''\Lambda=1|\beta_D' L_+|B\Lambda=0\rangle. \tag{13}$$

C. Fitting procedure

We present two fits here; the first, is a straightforward fit to the parameters determined directly by the data. The second fit, described in Sec. IV D, includes several estimated parameters to take account of interactions that are not directly observed. These other interactions are large enough to have a significant effect on the determined parameters, so the end result is a more physically reasonable set of values.

All the parameters which could be directly determined by the data were simultaneously varied in least-squares fits of calculated against observed data, until the best fit possible was obtained. The excited energy levels were calculated using large basis sets containing all the excited state levels of a given parity and J including the B states $v'=0$–6 as well as the B'' states $v'=2$–12. The ground state levels were calculated similarly using matrices containing all states of a given J and parity for $v''=0$–5 and 7. This simultaneous calculation is not required for the ground state levels, but it removes the need for extra programming. Despite the large numbers of parameters floated few problems with convergence of the fits were encountered. The only problems were with B $v'=6$ and B'' $v'=12$ where one or two parameters had to be varied manually to find the best value for the parameter and its error. This probably reflects the relatively small number of levels measured for B $v'=6$.

TABLE III. Comparison of fits to the $B\ ^3\Sigma_u^- v'=1$ state and the $B''\ ^3\Pi_u v'=3$ and 4 states. Figures in parentheses are three standard deviations.

				Patiño and Barrow[c]	
		Local fit[a]	Global fit[b]	e levels	f levels
$T_{v,0}$ (cm^{-1})	$Bv'=1$	32 114.12 (20)	32 102.71(23)		
	$B''v'=3$	32 035.55 (10)	32 039.70(13)		
	$B''v'=4$	32 342.149 (63)	32 344.732(53)		
B' (cm^{-1})	$Bv'=1$	0.221 145 (48)	0.223 429(80)	0.221 90(30)	0.221 54 (9)
	$B''v'=3$	0.201 72 (10)	0.201 702(79)	0.206 6 (12)	0.197 9(192)
	$B''v'=4$	0.200 405 (63)	0.199 143(84)	0.202 28(12)	0.201 1 (36)
λ' (cm^{-1})	$Bv'=1$	4.922 (90)	4.724(75)		
	$B''v'=3$	8.942 (90)	5.88(12)		
	$B''v'=4$	7.077 (45)	5.624(36)		
A' (cm^{-1})	$B''v'=3$	195.815 (69)	193.698(94)		
	$B''v'=4$	192.561 (81)	190.986(57)		
α (cm^{-1})	$B-B''(1-3)$	−7.51 (54)	18.43(29)		
	$B-B''(1-4)$	10.810 (96)	−11.291(60)	−12.15 (10)	12.26 (6)
β (cm^{-1})	$B-B''(1-3)$	−0.125 0 (60)	−0.080 8(18)	−0.0598 (6)	−0.0852 (11)
	$B-B''(1-4)$	−0.018 4 (18)	0.029 55(97)	−0.034 (6)	−0.0272 (2)
p (cm^{-1})	$B''v'=3$	0	0	1.2 (6)	
	$B''v'=4$	0	0	1.695 (18)	
q (cm^{-1})	$B''v'=3$	0	0	−0.034 9 (18)	
	$B''v'=4$	0	0	−0.003 7 (4)	

[a] Fit to these three states only.

[b] From the global fit to all B and B'' states (Tables VIII–XII).

[c] Reference 11. This fit calculated individual B'' components separately so the $T_{v,0}$, λ, and A values are not directly comparable.

As the Hamiltonian matrix becomes rather large when all the states are included the computational time becomes significant. For the 3320 transitions included in the final fit, approximately 200 independent diagonalizations are required (two parities for J up to 100 in the upper and lower states) and each calculation must be repeated for each parameter (171 times) to calculate the numerical derivatives. For this reason, use was made of a parallel computer, a Meiko Computing Surface 2. This computer is a distributed memory system, essentially several independent computers (6–8 were used for this work), so the calculation must be split into several independent parts with minimal communication between them. Fortunately this is easy to do for this calculation; work on each Hamiltonian matrix in one cycle of the least-squares fitting process can take place independently of the calculation on all the other matrices. Thus, given n matrices to diagonalize, the matrices are distributed equally over the p processors so that each processor calculates n/p levels. The results are then combined on one processor to do the least-squares correction. Given that this latter step is a small part of the total computational time, a speed up relative to a single processor close to p is obtained. In principle the repeated calculations to find the numerical derivatives could also be split over different processors, though this is not done here as the calculation is already split into enough parts. The only potential problem is in the distribution of the matrices over the processors, as there is a considerable variation in size (from 8 for f parity ground states to 53 for e parity excited states), implying a considerable variation in calculation time. This is overcome in the distribution logic by working through the states in order of J (varying fastest) then e/f then upper/lower state.

The significant computational effort invested in calculating all the states simultaneously is justified by obtaining more physically reasonable parameters which vary smoothly with vibrational state, and by requiring fewer parameters. This is due to two related effects: first, any given B'' state is typically close to two B state vibrational levels, so that the interaction with one B state level is changed by virtue of its interaction with the other. Second, some of the $B-B''$ perturbations, particularly the J-independent ones, are large enough to give measurable effects for levels more than one vibrational quantum away. These latter interactions with more distant states typically vary smoothly with J and could simply be modeled by an adjustment to the effective constants, though the effective constants would then be less easy to interpret.

The necessity for fitting all the states simultaneously may be illustrated by comparing constants obtained for a state deperturbed in a global fit with those obtained from an individual state fit. For example, if the $B\ v'=1$ state is deperturbed in isolation from the surrounding B states, only including interactions with the $B''\ v'=3$ and 4 states in the model, the constants obtained are different from those for the same state deperturbed in a global fit. The constants from both these fits are shown in Table III. Also given in Table III

TABLE IV. Deperturbed constants from fit 1 for the $Bv'=0-6$ states. Figures in parentheses are three standard deviations.

v'	$T_{v,0}$ (cm^{-1})	B' (cm^{-1})	D' (10^{-7} cm^{-1})	λ' (cm^{-1})	γ' (cm^{-1})
0	31 682.852(75)	0.224 201(53)	2.442(67)	2.877(96)	−0.0280(19)
1	32 108.69(23)	0.223 227(77)	2.72(10)	3.530(77)	−0.0185(12)
2	32 530.23(23)	0.222 105(84)	4.03(14)	2.42(13)	−0.0072(28)
3	32 947.82(17)	0.219 588(82)	3.21(13)	3.15(14)	−0.0028(29)
4	33 354.96(34)	0.219 83(15)	6.08(34)	3.45(19)	−0.0089(51)
5	33 768.55(22)	0.215 967(95)	3.35(22)	2.58(16)	−0.0009(39)
6	34 173.550(86)	0.213 37(11)	2.56(34)	1.42(19)	0.0029(25)

are the constants obtained by Patiño and Barrow[11] in their deperturbation of the $B\ v'=1$ state. In order to obtain a reasonable fit for this single state, they found it necessary to float the e and f parities separately and to include very large values of the Λ doubling parameters p and q for the B'' states.

The model described here does not require these Λ doubling parameters. These terms arise from the interaction of a Π state with distant Σ states to give a splitting between states of different parity. In the current case, we consider the interaction with the $B\ ^3\Sigma_u^-$ state directly, and the perturbations of the Π state could be viewed as an example of giant Λ doubling. In principle interactions with more distant Σ states would give rise to some additional shifts, but we estimate that these effects would be small, and in any case, could not be distinguished from the interactions with the several $B\ ^3\Sigma_u^-$ vibrational levels that are included as part of our global fit.

The degree to which each constant and perturbation could be determined by the data needed to be considered in some detail in order to establish whether or not it could be floated as a parameter in the fit. For example the parameter o, which gives the splitting between the 0^+ and 0^- components of the $^3\Pi_0$ state, had to be included to give a good fit for those vibrational levels where both components are observed. However, for most $B''\ \Omega=0$ levels only the e parity component was observed and so o could not be determined in these cases. The $^3\Pi_0 f$ component is rarely observed because of the $\Delta\Omega=0$ selection rule for the matrix elements of the spin–orbit perturbation, Eqs. (7) and (9). This means that the $B''\ \Omega=0$ levels can only gain intensity via mixing with the $\Omega=0$ component of the B state, of which only an e component exists. The f parity for the $\Omega=0\ B''$ state was only observed in those cases where a $B''\ \Omega=0$ level crossed a $B\ \Omega=1$ level (for which both e and f components exist). In the region of a crossing, the weak L-uncoupling perturbation [Eq. (8)] becomes significant and causes mixing of the two levels according to its selection rule $\Delta\Omega=\pm1$. The f parity component of the $B''\ \Omega=0$ state can therefore gain intensity in these cases by mixing with the f component of the $B\ \Omega=1$ state. Hence the value of o is only determined for the vibrational levels $v'=3$, 4, 7, and 10 where such crossings occur.

The same considerations are important in deciding which perturbations are determined. Whenever a $\Omega=0$ or 1 component of a B'' state crosses the $\Omega=0$ or 1 components of a B state, both the spin–orbit mixing term (α), and the L-uncoupling mixing term (β) would need to be included in the fit in order to model the avoided crossing. However, whenever a $\Omega=2$ component of a B'' state crosses a B state, the selection rules would allow mixing with the $\Omega=1$ component of the B state via the L-uncoupling mixing term, but the spin–orbit mixing would not be involved. Hence only β could be determined in this case.

The inclusion of the centrifugal distortion of the perturbation parameters in the fit also required similar considerations. The centrifugal distortion of the spin–orbit mixing (α_D) mixes states according to the selection rule $\Delta\Omega=0,\pm1$, whereas the centrifugal distortion of the L-uncoupling (β_D) obeys the selection rules $\Delta\Omega=0,\pm1,\pm2$. These selection rules restrict the parameters that have an effect in various cases. Furthermore, in order for these parameters to be determined for a particular interaction, there must be an avoided crossing between the two states at a high value of J. The number of cases for which α_D and β_D were required was therefore limited.

The sign of the matrix elements off-diagonal in electronic state are dependent on the phase convention chosen for the electronic wave functions (given above) and the vibrational wave functions. The absolute sign of the perturbation parameters is in any case not determined in our fit; changing the signs of all the perturbation parameters simultaneously makes no difference to the calculated energy levels or intensities. However several of the relative signs are determined by our fit; obviously if a pair of states is connected by more than one type of perturbation then the relative signs of the different perturbations are determined. If *both* these states are connected to a third state, then the relative signs of all the parameters interconnecting all three states are determined. In our model we do not have any sets of three states all interconnected in this way; however such connections do exist via fourth or fifth states. These indirect connections only have a very small effect on the model, so if, for example, the signs of the perturbations between one particular pair of B and B'' states are all changed then all the eigenvalues change, but by an amount less than our experimental error. We therefore chose to set the absolute signs of the α perturbation parameters so that they were consistent with the signs of the calculated vibrational overlap integrals between the B and the B'' states (with the vibrational wave function chosen such that the outermost lobe is positive). A more detailed model for α is developed below, which confirms this choice of signs.

TABLE V. Deperturbed constants from fit 1 for the $B''v'=2$–12 states. Figures in parentheses are three standard deviations.

v'	$T_{v,0}$ (cm^{-1})	B' (cm^{-1})	D' (10^{-7} cm^{-1})	A' (cm^{-1})	λ' (cm^{-1})	γ' (cm^{-1})	o' (cm^{-1})
2	31 725.55(10)	0.203 690(87)	3.82(19)	198.976(68)	5.343(94)	0.122(68)	0
3	32 038.62(13)	0.201 698(78)	3.99(11)	194.464(93)	6.34(12)	0.199(21)	2.40(20)
4	32 344.02(13)	0.199 359(90)	3.31(15)	191.409(88)	6.001(82)	0.063(12)	2.15(12)
5	32 640.158(73)	0.197 475(80)	3.82(15)	190.290(90)	5.342(85)	0.148(49)	0
6	32 931.19(13)	0.194 50(17)	3.35(23)	186.094(72)	4.98(11)	0.385(63)	0
7	33 216.35(18)	0.190 82(10)	2.11(31)	179.04(12)	4.52(13)	0.037(14)	0.39(23)
8	33 485.03(10)	0.189 64(23)	5.36(47)	177.53(15)	5.77(13)	0.074(67)	0
9	33 749.36(24)	0.186 51(24)	7.80(53)	170.66(15)	5.54(14)	0.28(13)	0
10	33 998.813(91)	0.184 33(15)	4.53(45)	165.60(11)	6.600(37)	−0.042(17)	1.50(18)
11	34 239.75(10)	0.179 20(30)	7.6(5)	156.94(13)	5.30(11)	0.343(70)	0
12	34 453.183(58)	0.177 47(10)	0	136.69(14)	0	0	0

Using considerations such as these a set of 172 parameters that are directly determined from our data was constructed, and a fit to these parameters (fit 1) produced constants and perturbation values given in Tables IV–VI. This gave a good fit, with a standard deviation of 0.064 cm^{-1}.

D. Parameter model

The drawback with fit 1 is that there are several parameters that we expect to be significant, but which cannot be determined from the data. For example, the α perturbation parameter will act between all B and B'' states with the same Ω component. However it can only be well determined between those states with avoided crossings. For those cases where states are close but do not cross the calculated energy levels will be changed by omission of this parameter. The changes can be dealt with by adjusting the values of other constants, but this will give difficulties in interpretation of these parameters. We therefore also provide an alternative fit, fit 2, in which as many as possible of the significant parameters are either floated or set to estimated values. The basis of the estimation is that the parameters in the Hamiltonian should show a smooth variation with r. The constants for the individual vibrational states should then show a smooth variation with v and it should also be possible to estimate the matrix elements connecting the different vibronic states from the vibrational wave functions. This is part of the way toward directly fitting the underlying B and B'' potential energy curves and r-dependent electronic interaction parameters rather than the individual fine-structure constants for each state.

TABLE VI. Perturbations determined from fit 1. Figures in parentheses are three standard deviations.

$Bv'-B''v'$	α (cm^{-1})	α_D (10^{-4} cm^{-1})	β (cm^{-1})	β_D (10^{-6} cm^{-1})
0–2	14.699(71)	2.69(45)	−0.0414(63)	−1.27(50)
0–3	−4.65(37)	−6.10(58)	−0.0635(87)	13.0(13)
1–3	18.36(29)	−7.0(14)	−0.0808(18)	⋯
1–4	−11.289(60)	−4.82(29)	0.0241(15)	1.70(39)
2–4	18.56(59)	−28.0(17)	−0.0497(30)	−22.3(31)
2–5	−15.35(11)	−3.71(29)	0.0492(62)	0.86(62)
2–6	10.77(23)	⋯	0.0240(43)	⋯
3–6	−17.980(81)	⋯	0.0776(68)	⋯
3–7	11.16(22)	7.11(74)	0.0066(55)	−11.8(18)
4–7	−25.27(49)	26.4(26)	0.0369(24)	⋯
4–8	14.78(14)	1.47(53)	−0.0514(53)	⋯
5–9	16.29(11)	⋯	−0.069(12)	⋯
5–10	−11.59(21)	−5.1(11)	−0.0037(48)	13.3(22)
6–10	⋯	⋯	−0.0627(84)	⋯
6–11	−13.45(14)	−4.62(97)	0.0693(71)	⋯
6–12	11.84(25)	⋯	0.0237(20)	⋯

The parameters that need to be estimated are o, α, and β. Estimating the parameter o is straightforward as it should show a smooth variation with vibrational state. We assumed a linear relationship with v, which reproduced the observed values to 0.4 cm^{-1}.

The modeling of the perturbation parameters is not so straightforward but, as suggested above, is actually rather important as interactions with states more than one vibrational quantum away can be significant. The parameters to be determined are the matrix elements between *vibronic* states, such as

$$\alpha=\langle B''\Lambda=1,v''|(\tfrac{1}{2}A+B)\hat{L}_+|B\Lambda=0,v\rangle. \tag{14}$$

If we initially assume that the electronic operator mixing the two states is independent of r then the parameter will be proportional to the overlap of the vibrational wave functions,

$$\alpha=\langle v''|v\rangle\langle B''\Lambda=1|(\tfrac{1}{2}A+B)\hat{L}_+|B\Lambda=0\rangle. \tag{15}$$

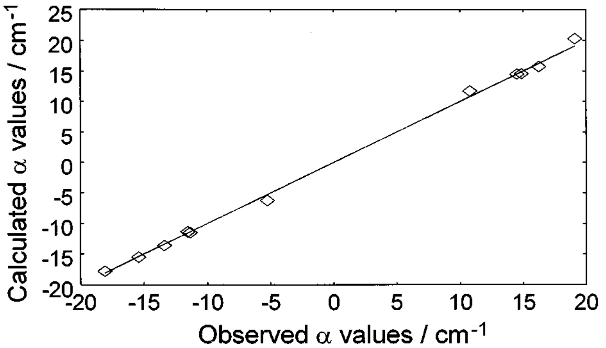

FIG. 9. Plot of observed α values against those calculated from Eq. (15) using the parameters in Table IX. The experimental errors in α are less than the size of the points.

TABLE VII. Coefficients from least-squares fit of observed against calculated α and β values using Eq. (16) with $r_e=2$ Å. Figures in parentheses are one standard deviation.

Coefficients	α	β
a_0/cm^{-1}	29.9 (1.4)	−0.126 (52)
a_1/cm^{-1} Å^{-1}	187 (24)	−3.33 (56)
a_2/cm^{-1} Å^{-2}	−421(110)	

TABLE IX. Calculated β parameters (in cm^{-1}) set as fixed values in fit 2.

	$B''v$			
Bv	5	8	9	12
1	−0.004			
3	−0.051	0.003		
4			0.009	
5		0.039		
6				−0.008

We therefore calculated the Franck–Condon factors between the B'' and B states from our data. This required deriving RKR potentials for both the B and the B'' states from our experimentally determined rotational and vibrational constants, using the program AAEE.[25] The program LEVEL[26] was then used to generate vibrational wave functions from the RKR potentials for both states and also the Franck–Condon factors between the vibrational levels of the two potentials.

These calculated Franck–Condon factors were found to be broadly proportional to the measured α values. However by including an r dependence in the electronic operator a better fit could be obtained, i.e., by modeling the α values as

$$\alpha=\langle v''|a_0+a_1(r-r_e)+a_2(r-r_e)^2|v\rangle. \tag{16}$$

A small least-squares program was written to find the best values of the coefficients a_0, a_1, and a_2 using the vibrational wave functions from LEVEL and the values of α that were well determined by the line position fit. This gave an excellent fit to the α values (average error 0.36 cm^{-1} in parameters of 10–20 cm^{-1}), as shown by Fig. 9.

The coefficients obtained from the least-squares fit to Eq. (15) against observed values of α are given in Table VII below. Using this polynomial, the α values for all the possible $B''-B$ pairs could then be calculated and included in the fit as fixed parameters. These calculated values of α are given Table VIII. It is clear from these calculations that the interactions between $B''v=0$ and 1 and $Bv=0$ and 1 are significant as the matrix elements between them are large. For this reason the $B''v=0$ and 1 were included in fit 2, although they were not observed experimentally and their positions had to be estimated by extrapolating the origin, B, A, and λ from the higher states.

A similar analysis was performed for the β perturbation parameters, in this case using a fit weighted by the uncertainty in the experimental β values. This was deemed necessary as the errors in the β values were significantly larger than for the α values. This fit was not as satisfactory (average error 0.009 cm^{-1} in parameters of ~0.01–0.06 cm^{-1}) though the correct sign is predicted for all except one case ($B0-B''3$). This and three other points that were modeled poorly were excluded from the fit. For the β values a reduced precision in the fit compared to the fit to the α values is acceptable since the β perturbations are so weak except at high J. Their long-range effects are thus negligible and very few need to be included as fixed values in the fit. The coefficients for the least-squares fit of calculated against observed β values are given in Table VII, and the calculated β values that were included in the fit are given in Table IX.

The calculated values of α, β, and o were then held fixed while allowing the same parameters as before to float. The entire process of estimating parameters was iterated several times as the parameters from the revised fit were used to produce a new estimate of the undetermined parameters. The final fit, fit 2, has a standard deviation of 0.064 cm^{-1}, essentially the same as the previous fit. However, the molecular constants for this fit, given in Tables IX–XI, show a smoother variation with vibrational state than both the previous fit and the constants prior to deperturbation. An example of this can be seen in Fig. 12(a) where three sets of B'' state origins are plotted against vibrational state. The highest state in our fit, $v'=6$ for the B state and $v'=11$ and 12 for the B'' state are necessarily only partially deperturbed in our fit as we have excluded higher states, though the parameters derived from these states seem on the whole to be in line with those of other states.

To complete the model, some of the ground state constants for $v''=2$–4 and 7 were also floated as our data allowed a better determination of these constants. The values for $v''=0$ and 1 were not floated as they are better deter-

TABLE VIII. Calculated α parameters (in cm^{-1}) set as fixed values in fit 2.

	$B''v$												
Bv	0	1	2	3	4	5	6	7	8	9	10	11	12
0	36.27	−27.27			2.15	−0.49							
1	28.54	11.78	−25.45			4.90	−1.51	0.10					
2			−6.50	−16.78	21.33		8.28	−3.26	0.65				
3			17.87	−16.66	−5.68	18.17			−5.72	1.78	0.19		
4						4.86	11.76	−17.47		−8.63	3.59	−0.48	
5							12.63	3.56	−14.36			6.03	−1.79
6									−4.65	−9.51	14.88		8.80

mined from the Fourier transform infrared data.[21] The final values, given in Table XII, are consistent with previous values.[16]

Full details of both fits, including a tabulation of both the observed and calculated line positions and a correlation matrix for the determined parameters is available from the authors. As mentioned above, both fits reproduce all the 3320 observed transitions well, with a maximum error of 0.4 cm^{-1}. The greatest discrepancies are typically at the highest observed J for a particular state, where we do not model in detail crossings at still higher values of J.

The error bars given in the tables are taken directly from the least-squares fits. However, for fit 2 we must consider possible systematic errors due to uncertainties in the estimated parameters and truncation of the vibronic basis. For example, our model for the α perturbation parameters reproduced the measured values to $\pm 0.36\ \mathrm{cm}^{-1}$. If a change is made to any one of the estimated α values of 0.36 cm^{-1} and fit 2 repeated, the largest change seen is in the origins of the states connected by that particular parameter, and is less than twice the quoted error bars for the origins. A similar procedure for the β perturbation parameters also found the largest changes in the other parameters to be within the original error bars. Our estimation of the position of the $B''v'=0$ and 1 levels also has an effect on the constants we determine, but again the effect is small. A change in the origin of $B''v'=1$ by 10 cm^{-1} produces changes of 0.01 cm^{-1} in λ and 0.2 cm^{-1} in the origin for $Bv'=0$. The estimated parameter with the greatest uncertainty is o, as an adjustment in this parameter feeds through directly to a correction to the origin, A, and λ for the B'' state involved. However, our estimates for o are less precise than for the other estimated parameters, leading to a possible systematic error in the origin, A, and λ for the B'' states up to 0.4 cm^{-1}. The effect of this uncertainty on the other parameters will be less than their error bars as for α and β.

We can apply a similar procedure to estimate the effect of truncating the vibronic basis at $v'=6$ for the B state and $v'=12$ for the B'' state. We comment above that interactions with $B''v'=0$ and 1 are large and these states are therefore included in the basis. Their omission leads to changes of 2 cm^{-1} in λ and 10 cm^{-1} in the origin for $v'=0$ of the B state. This is an extreme case as our calculations (Table VIII) reveal that the 0–0 matrix element is the largest and the higher v levels have smaller matrix elements. We nevertheless expect some truncation errors for $v'=6$ for the B state and $v'=12$ for the B'' state and possibly for lower states. Determination of these must await analysis of the higher vibronic levels.

It should be emphasized that both the basis truncation errors and the parameter estimation errors do not affect the calculated position of any of the observed levels but only the prediction of the unobserved levels.

E. Lifetimes

The work of Matsumi *et al.*[14] suggested that there was no intrinsic intensity to the B'' state, and so the intensity of any B'' transition was due to mixing in of B state character. This mixing can be calculated from our model, and thus intensity measurements can give an independent check on our model. It is difficult to measure absolute intensities of different vibrational bands using laser-induced fluorescence, but equivalent information can be obtained from the fluorescence lifetimes of the states concerned. The excited state can only fluoresce to the ground state so the lifetime should be inversely proportional to the B character of each state (assuming the transition moment is independent of r):

$$\tau_f \propto 1 \bigg/ \sum_i \, (c_i^2), \tag{17}$$

where c_i is the coefficient of the ith state in our basis in the actual state and the sum extends over only the B states in the basis. This sum will depend on J as well as Ω and v, but as the mixing in the low J levels for which lifetimes were measured is dominated by the J-independent spin–orbit perturbation the choice of J is not normally important.

In fact Matsumi *et al.*[14] derived homogeneous spin–orbit matrix elements from their lifetime data and band positions by using a model containing two or, in some cases, three

TABLE X. Deperturbed constants from fit 2 for the $B''v'=0$–12 states. Figures in parentheses are three standard deviations.

v'	$T_{v,0}$ (cm^{-1})	B' (cm^{-1})	D' ($10^{-7}\ \mathrm{cm}^{-1}$)	A'	λ'	γ'	o'
0	31 069[a]	0.208[a]	3.5[a]	198.5[a]	5.5[a]	0[a]	2[a]
1	31 402[a]	0.206[a]	3.5[a]	197.5[a]	5.5[a]	0[a]	2[a]
2	31 729.27(10)	0.203 549(88)	3.74(19)	195.315(67)	5.237(91)	0.105(66)	1.7[a]
3	32 039.70(13)	0.201 702(79)	4.04(12)	193.698(94)	5.88(12)	0.191(21)	1.36(20)
4	32 344.732(53)	0.199 143(84)	3.27(15)	190.986(57)	5.624(36)	0.048(11)	1.681(96)
5	32 642.155(68)	0.197 315(80)	3.79(15)	188.430(90)	5.165(76)	0.190(40)	1.2[a]
6	32 933.03(16)	0.194 41(17)	3.25(25)	184.203(93)	5.07(11)	0.486(68)	1.0[a]
7	33 214.074(67)	0.190 66(11)	0.65(38)	180.324(68)	6.021(30)	0.059(14)	1.60(14)
8	33 486.19(12)	0.189 71(24)	5.53(48)	176.54(18)	5.52(15)	0.113(67)	0.6[a]
9	33 749.22(24)	0.186 31(24)	7.42(55)	170.85(15)	5.49(14)	0.27(13)	0.4[a]
10	34 000.272(90)	0.184 03(15)	4.33(46)	164.76(10)	5.794(38)	−0.022(17)	0.21(18)
11	34 239.34(12)	0.178 89(31)	6.5(15)	157.36(12)	5.32(13)	0.149(89)	0.1[a]
12	34 460.292(43)	0.176 09(48)	−10.1(21)	148.484(55)	5.5[a]	0.0[a]	0.0[a]

[a] Estimated values; see the text.

TABLE XI. Deperturbed constants from fit 2 for the $Bv'=0$–6 states. Figures in parentheses are three standard deviations.

v'	$T_{v,0}$ (cm^{-1})	B' (cm^{-1})	D' (10^{-7} cm^{-1})	λ' (cm^{-1})	γ' (cm^{-1})
0	31 672.426(77)	0.224 647(54)	2.571(68)	4.591(96)	−0.0324(19)
1	32 102.71(23)	0.223 429(80)	2.75(11)	4.724(75)	−0.0226(11)
2	32 525.644(34)	0.222 471(74)	4.35(13)	3.42(11)	−0.0036(22)
3	32 943.80(18)	0.219 572(83)	3.03(14)	3.88(14)	0.0022(32)
4	33 359.406(85)	0.219 52(16)	6.74(53)	2.99(23)	−0.0098(52)
5	33 766.65(22)	0.216 068(96)	3.16(22)	2.96(16)	0.0035(39)
6	34 170.925(54)	0.214 02(13)	3.24(39)	1.12(15)	−0.0133(38)

interacting states. The matrix elements they derive from this simple model are consistent with ours, though their error bars are larger as the lifetime data are less precise. This is shown by Fig. 10, where the matrix elements from the two models are plotted against each other. In Fig. 11 we plot the lifetimes measured in our work as well as those of Matsumi *et al.*[14] against our calculated B state character for $\Omega=0$ and 1 states. The linearity of these plots demonstrates that Eq. (17) holds for both the B and B'' states and the assumption of an r-independent transition moment is reasonable. The intercept (at 100% B character) of these plots at 32±1 ns gives the lifetime of a pure B state.

This model would predict a very low intensity for the $\Omega=2$ components of the B'' state. This is because the $\Omega=2$ components can only mix with the B state via the L-uncoupling mixing term [Eq. (6)], which obeys selection rules $\Delta\Omega=1$ and is $\sim10^3$ times weaker than the spin–orbit term for low J. Our model predicts a B state character of 10^{-5} in typical $\Omega=2$ states, corresponding to a lifetime of ~3 ms. Our observations indicated that transitions to the $\Omega=2$ states were indeed weak, requiring higher laser powers than the $\Omega=0$ or 1 components, but the lifetimes of ~4 μs indicate that there is in fact a small transition moment direct to the B'' state. It is sufficiently weak that it will not alter the model above for the stronger transitions. In principle this means that it should be possible to observe transitions to the f parity $\Omega=0$ levels but these are always coincident with the much stronger e parity $\Omega=0$ levels and therefore difficult to observe.

We can now use our model to calculate the intensity of all the individual rovibronic transitions. The relative intensities of the B–X bands are available as Franck–Condon factors from the work of Anderson *et al.*[18] The direct B''–X contributions are included by using Franck–Condon factors calculated from the known wave functions for the B'' and X states. These must be scaled down by the ratio of electronic transition moments which we estimate from the state lifetimes; for the B state we use the 32 ns calculated above and for the B'' state we use 4160 ns, the average of our measurements. The relative intensities within each band, and the intensity arising from the B''–B mixing are calculated from the wave functions given by our model. This process also gives the lifetime of each rotational state. A table of calculated line strengths, positions, and upper state lifetimes is available from the authors.

These calculated line strengths and positions should be adequate to describe experimental spectra of the B and B'' states up to our highest observed J for each vibrational state. However several points should be noted when using the calculated line strengths in conjunction with experimental methods. No corrections should be needed for simple absorption measurements, but if laser-induced fluorescence is used then

TABLE XII. Perturbations determined from fit 2. Figures in parentheses are three standard deviations.

Bv'–$B''v'$	α (cm^{-1})	α_D (10^{-4} cm^{-1})	β (cm^{-1})	β_D (10^{-6} cm^{-1})
0–2	14.874(70)	2.50(45)	−0.040 4(62)	−1.08(50)
0–3	−5.02(38)	−5.51(60)	−0.052 5(89)	11.5(13)
1–3	18.43(29)	−7.6(14)	−0.080 8(18)	⋯
1–4	−11.291(60)	−4.88(29)	0.029 55(97)	⋯
2–4	⋯	−29.3(13)	−0.041 1(21)	−26.9(20)
2–5	−15.27(10)	−3.79(29)	0.056 6(39)	⋯
2–6	⋯	3.61(32)	0.017 1(47)	⋯
3–6	−18.088(85)	⋯	0.086 2(80)	⋯
3–7	10.69(21)	8.30(71)	−0.002 9(58)	−9.6(19)
4–7	⋯	48.1(42)	0.050 9(61)	6.2(36)
4–8	14.49(16)	2.43(50)	−0.027 9(68)	−5.4(16)
5–9	16.24(12)	⋯	−0.067(13)	⋯
5–10	−11.36(22)	−6.3(11)	0.000 7(51)	12.1(24)
6–10	⋯	⋯	−0.033 7(77)	⋯
6–11	−13.41(16)	−5.74(96)	0.055 0(94)	⋯
6–12	13.35(40)	⋯	⋯	⋯

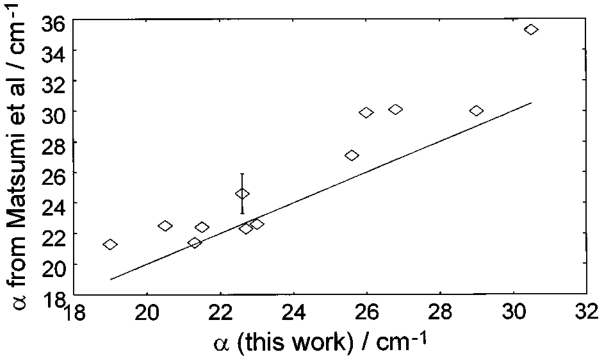

FIG. 10. Plot of matrix elements determined in this work (fit 2) against matrix elements calculated by Matsumi *et al.* (Ref. 14) from lifetime data. The line $y=x$ is plotted to show the expected relationship. A sample error bar of one standard deviation is given for the matrix elements of Matsumi *et al.* (Ref. 14), estimated from errors in their measured lifetimes. The errors in fit 2 are negligible on the scale of the plot.

the varying lifetime of the upper states can affect the observed intensity. If all the fluorescence is collected there is no problem, but a typical experiment will sample the fluorescence over a finite time interval or there could be collisional quenching of the fluorescence. Both of these factors will usually discriminate against the longer lived states so a correction must be applied. The lifetime of the upper state involved in each transition can be calculated from our model, and is included in our table, so if the other factors are known the correction can be calculated. Alternatively the tables can be used to select lines with a reasonably constant upper state lifetime. Note that our room temperature spectra (Figs. 5 and 6) were necessarily taken at pressures where there would be significant fluorescence quenching, so we do not expect quantitative agreement between the simulated and observed intensities, though the match is reasonable.

V. DISCUSSION

Due to the strong perturbations in the system, many of the molecular constants for the B and B'' states before deperturbation varied irregularly with vibrational quantum number. This is because the constants were evaluated assuming no interactions between the two electronic states. However, by including the interactions in the model, the deperturbed constants obtained varied smoothly with vibrational quantum number, following simple analytical expressions as expected.

As shown earlier [Fig. 12(a)] the origins for the B'' state vary more smoothly with vibrational level after deperturbation than before, with fit 2 showing a smoother trend than fit 1. The difference in the behavior of the constants before and after deperturbation is perhaps most dramatic for the spin–spin splitting constant λ for the B state shown in Fig. 12(f), which behaved erratically before deperturbation, changing sign a number of times between with increasing vibrational level, as shown by Meyer and Crosley[8] and Matsumi *et al.*[13] Since the splitting between the $\Omega=0$ and $\Omega=1$ components of the $B\ ^3\Sigma_u^-$ state is approximately 2λ, a shift in energy of either component would cause the effective value of λ to change. A shift such as this would be caused by the presence of a nearby $\Omega=0$ or $\Omega=1$ component of a B'' state which would interact with the B state via the homogeneous spin–orbit interaction. The value of λ for the B state would therefore vary depending on which B'' states were close to it and whether they lay at higher or lower energy. However, after the interactions were included in the model, the deperturbed value of λ showed little variation with vibrational level. We also give in Fig. 12 plots of band origins and B values for the B state, and A and B values for the B'' state. These plots show that all of the deperturbed constants follow smooth trends when compared to the values before deperturbation.

The plots in Fig. 12 show that the deperturbation procedure, in addition to smoothing the vibrational state dependence of the constants, also shifts some of them by significant amounts. Note for example the rotational constants for the B states which are consistently shifted down with respect to the deperturbed values, while the band origins lie on either side of the deperturbed values. The reasons for this behavior can be seen by considering just the J-independent mixing between the states which is normally dominant. Second-order perturbation theory indicates that this will shift the origins of the states by $\pm\alpha^2/\Delta$ where Δ is the separation between states, depending on whether the interacting state is above or below the B state. However this interaction will

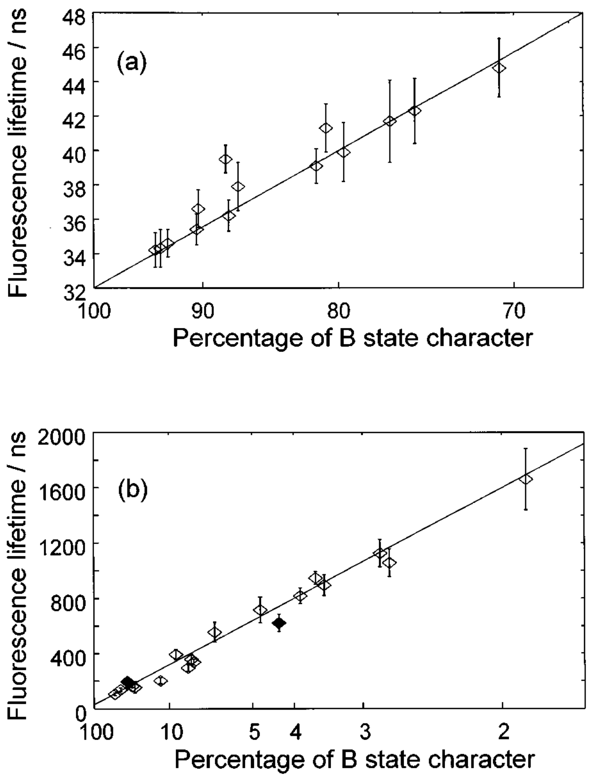

FIG. 11. Fluorescence lifetimes (τ_f) of (a) the B states and (b) the B'' states plotted against percentage of B state character calculated according to $\Sigma_i(c_i)^2$ where c_i are the coefficients of the B state basis functions. The nonlinear scale arises because τ_f is inversely proportional to $\Sigma_i(c_i)^2$ as given in Eq. (17). The two filled symbols are lifetimes measured in this work and the remainder are lifetimes measured by Matsumi *et al.* (Ref. 14). The B'' $\Omega=2$ components are not included in these plots.

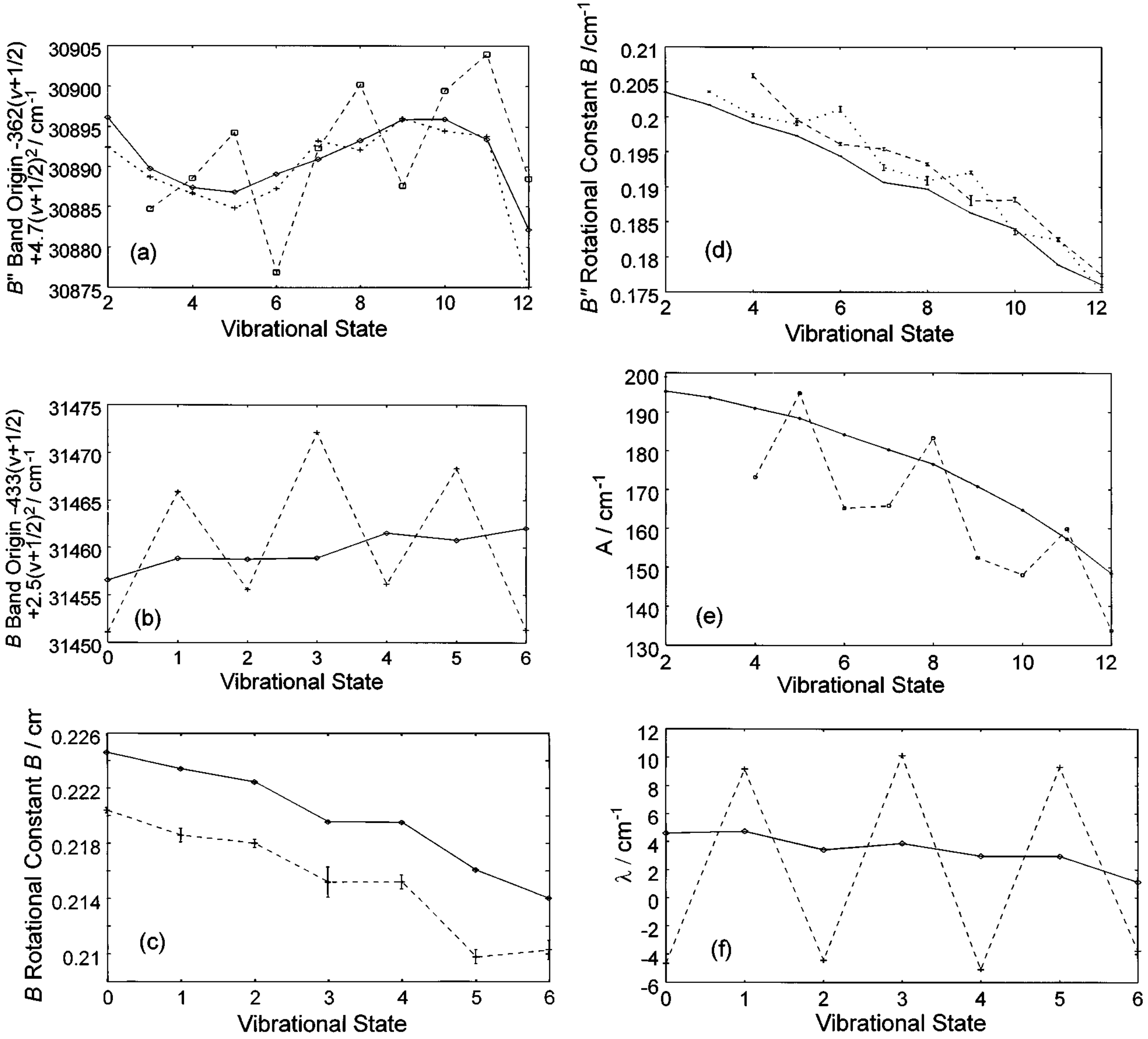

FIG. 12. Graphs of molecular constants before and after deperturbation against vibrational state. The constants before deperturbation (dashed lines) are taken from Matsumi *et al.* (Ref. 13) and the constants after deperturbation (solid lines) are taken from this work (fit 2). (a) Band origins for the B'' state. The dotted line represents the values after deperturbation using fit 1. The Matsumi data have been shifted down by 342 cm^{-1} to correct for a difference in definition of the band origins. (b) Band origins for the B state. (c) Rotational constants for the B state. (d) Rotational constants for the B'' state. For the Matsumi *et al.* data (Ref. 13) values for both the $\Omega=0$ (dashed line) and the $\Omega=1$ (dotted line) states are plotted. (e) Spin–orbit splitting constants (A) for B'' state. (f) Spin–spin splitting constants (λ) for the B state.

also cause a correction to B as the separation between the states, Δ, changes with J as the rotational constants in the B and B'' states differ. The correction to the energy of the B state is of the order of

$$\frac{\mp\alpha^2}{\Delta} = \frac{\mp\alpha^2}{|\Delta_0| \pm (B_{B''}-B_B)J(J+1)}$$
$$\approx \mp\frac{\alpha^2}{\Delta_0} - \frac{\alpha^2}{\Delta_0^2}(B_B-B_{B''})J(J+1), \qquad (18)$$

where Δ_0 is the energy difference between the interacting B and B'' levels at $J=0$. The upper signs correspond to a B'' level situated above a B level, and the lower signs correspond to a B'' level below a B level. It can be seen from this equation that although the sign of the correction to the band origin changes, the sign of the correction to B is always negative. This is because a B'' state below a B state will raise the lower J states, lowering the effective value of B, while a B'' state above will depress the higher J states, again lowering the effective value of B.

A slight discontinuity appears in the B state rotational constant around the levels $v'=3$ and $v'=4$ as well as in the B'' constants of B and D which show irregularities at $v'=7$. These irregularities may be caused by another electronic state in this region perturbing either the B or the B'' states. There are three known states of u symmetry below the B and B'' states, the $A'\ ^3\Delta_u$, $A\ ^3\Sigma_u^+$, and $c\ ^1\Sigma_u^-$ states,[27,28] all three of which could perturb the $B''\ ^3\Pi_u$ state via spin–orbit mixing. The origins of these states lies some 10 000 cm^{-1} below the B and B'' states, so only the high vibrational levels of the A, A', and c states can give any effect. The vibrational overlap between the states will therefore be small so perturbations will only be significant where there is a close resonance between the energy levels. This is consistent with our observation of a single irregularity.

Since this deperturbation analysis only involves the vibrational levels of the B state $v'=0$–6 and the B'' $v'=2$–12, interactions between the B $v'=6$ and higher B'' states as well as those between B'' $v'=12$ and higher B states have not been included. The highest B and B'' vibrational levels in this work are therefore only partially deperturbed and the constants for the states should be treated as preliminary. This has led to anomalous values for their constants. For example, the deperturbed value of λ for the B state $v'=0$–5 ranges between 3.0 and 4.6, whereas the value for $v'=6$ is 1.1.

VI. THE MOLECULAR CONFIGURATION QUESTION

During this work, uncertainties about the molecular configurations of the B and B'' states became apparent. Of the few *ab initio* calculations performed on S_2, those by Swope *et al.*[29] remain the most relevant to this work. They carried out self-consistent field and configuration interaction type calculations on several low lying bound states of S_2, including the B and B'' states, predicting that the B'' state lay about 400 cm^{-1} below the B state. The accepted configurations of the three states as given by Swope *et al.*[29] are as follows:

$$B\ {}^3\Sigma_u^- \quad \cdots 5\sigma_g^2 2\pi_u^3 2\pi_g^3, \tag{19}$$

$$B''\ {}^3\Pi_u \quad \cdots 5\sigma_g^2 2\pi_u^4 2\pi_g^1 5\sigma_u^1, \tag{20}$$

$$X\ {}^3\Sigma_g^- \quad \cdots 5\sigma_g^2 2\pi_u^4 2\pi_g^2. \tag{21}$$

The relative intensities of the $B-X$ and $B''-X$ transitions predicted from these configurations agree well with experiment. As discussed by Herzberg[30] and Mulliken,[31,32] a parallel transition from a bonding π_u orbital to the corresponding antibonding π_g orbital, such as for the $B-X$ transition, should have considerable intensity. However, a transition involving a π to σ promotion, such as for the $B''-X$ transition, where the transition moment is perpendicular to the internuclear axis and the electron goes from one antibonding orbital to another antibonding orbital, is expected to have a much lower transition dipole moment. This is consistent with the relative transition dipole moments estimated from fluorescence lifetime measurements in this work.

However, interpretation of the data presented in this work has established that there is strong spin–orbit mixing between the B and B'' states, which would not be possible with these configurations. For any mixing to occur via the one electron spin–orbit operator, the B and B'' molecular configurations must differ by only one spin orbital. This problem could be overcome by including an additional configuration for either the B or the B'' state and, in fact, Swope *et al.*[29] point to significant configuration interaction between the configuration for the B state given above with

$$\cdots 5\sigma_g^1 2\pi_u^4 2\pi_g^2 5\sigma_u^1 \quad ({}^3\Sigma_u^-). \tag{22}$$

This would give a nonzero interaction matrix element with the B'' configuration shown above. It is also possible to get configuration interaction in the B'' state and, while this is not considered explicitly by Swope *et al.*, configuration mixing is found in both of the analogous states in O_2.[33] Mixing with the configuration:

$$\cdots 5\sigma_g^2 2\pi_u^2 2\pi_g^3 5\sigma_u^1 \quad ({}^3\Pi_u) \tag{23}$$

would give spin–orbit interaction with configuration (19) and would if anything reduce the $B''-X$ transition dipole moment from the ground state as the transition $5\sigma_g^2 2\pi_u^2 2\pi_g^3 5\sigma_u^1 - 5\sigma_g^2 2\pi_u^4 2\pi_g^2$ is orbitally forbidden.
The matrix elements between the various states can be estimated using the methods discussed by Lefebvre-Brion and Field[22] (Sec. 2.4.2) by expressing the spin–orbit operator in its many electron form,

$$\hat{H}_{\mathrm{SO}} = \sum_i a \hat{\mathbf{l}}_i \cdot \hat{\mathbf{s}}_i . \tag{24}$$

The single electron spin–orbit coupling constant a, may be estimated at around 340 cm^{-1}, given spin–orbit coupling constants in the B'' state of around 170 cm^{-1} (see Table X). The spin–orbit matrix elements between the various configurations work out at $0.15a-0.35a$, depending on the exact states involved, and so our observed values of α can be accounted for with configuration mixing of the order of 5%–35%. As the observed α values are r dependent, the mixing is also presumably r dependent. This is born out by the significant variation in A with v, suggesting the configuration of the B'' state changes with r.

To shed more light on the configuration we performed some multireference configuration interaction calculations using MOLPRO.[34] Using a large basis set (AVQZ) we could reproduce the form of the potential energy curves around the equilibrium region quite accurately, though there was significant deviation from the RKR curves above 2.6 Å. The calculation gave transition dipole moments at 2.3 Å of 1.91 D for $B-X$ and 0.090 D for $B''-X$, corresponding to lifetimes of 27 ns and 12 μs, in reasonable agreement with our observations of 32 ns and 4.16 μs. The same calculation gave the following natural orbital occupancies:

	$5\sigma_g$	$2\pi_u$	$2\pi_g$	$5\sigma_u$
$B\ {}^3\Sigma_u^-$	1.73	3.08	2.80	0.28
$B''\ {}^3\Pi_u$	1.92	3.55	1.39	1.03

These are consistent with both states undergoing significant configuration mixing, along the lines suggested above.

VII. CONCLUSIONS

A model of the interacting $B\ {}^3\Sigma_u^-$ ($v'=0$–6) and $B''\ {}^3\Pi_u$ ($v'=2$–12) states is presented here which fits the positions of the 3320 experimentally measured lines to 0.064 cm^{-1}. This deperturbation analysis was carried out by a simultaneous variation of all the constants and perturbations defined by the data in appropriate Hamiltonian matrices. The deperturbed constants obtained vary smoothly with vibrational number except for discontinuities in the constants between B state levels $v'=3$ and 4, which we attribute to weaker interactions with other states.

Fluorescence lifetimes were measured for the B'' states and were found to be consistent with those of Matsumi *et al.*[14] These lifetime measurements provide an independent verification of the state mixing in the system thereby confirming our model. Measurements of the fluorescence lifetimes of the previously unseen $\Omega=2$ components of the B'' state indicate a small intrinsic $B''-X$ transition strength. This allows us to construct a comprehensive model for the intensities as well as the positions of all the rovibronic transitions.

The molecular configurations of the states involved have been investigated and indicate configuration mixing for both the B and B'' states. Preliminary calculations using the program MOLPRO have been carried out which support this proposal as well as predicting transition dipole moments for the two states which are consistent with experiment.

ACKNOWLEDGMENTS

We would like to thank the EPSRC for funding a studentship for M.E.G., and providing the parallel computer and laser equipment used in this work. We are particularly grateful to Dr. R. F. Barrow (Oxford) and his group including Dr. J. M. Ketteringham, Dr. H. J. Hurst, Dr. J. M. Ricks, and Dr. P. Patiño for providing details of their data and analyses. We would also like to thank Gabriel Balint-Kurti for helpful discussions and assistance with the *ab initio* calculations and Keith Rosser for help with the equipment.

[1] J. I. Graham, Proc. R. Soc. London Ser. A **84**, 311 (1910).
[2] S. P. Sapers and D. J. Donaldson, J. Chem. Phys. **94**, 8918 (1990).
[3] N. van Veen, P. Brewer, P. Das, and R. Bersohn, J. Chem. Phys. **79**, 4295 (1983).
[4] K. S. Noll, M. A. McGrath, L. M. Trafton, S. K. Atreya, J. J. Caldwell, H. A. Weaver, R. V. Yelle, C. Barnet, and S. Edgington, Science **267**, 1307 (1995).
[5] J. M. Ricks and R. F. Barrow, Can. J. Phys. **47**, 2423 (1969).
[6] R. F. Barrow and R. P. du Parcq, in *Elemental Sulfur*, edited by B. Meyer (Interscience, New York, 1965), Chap. 13.
[7] J. E. Meakin and R. F. Barrow, Can. J. Phys. **40**, 377 (1962).
[8] K. A. Meyer and D. R. Crosley, Can. J. Phys. **51**, 2119 (1973).
[9] V. E. Bondybey and J. H. English, J. Chem. Phys. **69**, 1865 (1978).
[10] C. R. Quick and R. E. Weston, J. Chem. Phys. **74**, 4951, (1981).
[11] P. Patiño and R. F. Barrow, J. Chem. Soc. Faraday Trans. 2 **78**, 1271 (1982).
[12] M. Heaven, T. A. Miller, and V. E. Bondybey, J. Chem. Phys. **80**, 51 (1984).
[13] Y. Matsumi, T. Munakata, and T. Kasuya, J. Chem. Phys. **81**, 1108 (1984).
[14] Y. Matsumi, T. Suzuki, T. Munakata, and T. Kasuya, J. Chem. Phys. **83**, 3798 (1985).
[15] S. M. Harris, D. Phil. thesis, Oxford University, 1979; P. Patiño, D. Phil. thesis, Oxford University, 1983; Y. de Vita Villamizar, D. Phil. thesis, Oxford University, 1970; and unpublished data provided by J. M. Ketteringham, H. J. Hurst, R. F. Barrow, and co-workers.
[16] J. M. Ricks, D. Phil. thesis, Oxford University, 1970.
[17] K. N. Rosser, Q. Wang, and C. M. Western, J. Chem. Soc. Faraday Trans. **89**, 391 (1993).
[18] W. R. Anderson, D. R. Crosley, and J. E. Allen, Jr., J. Chem. Phys. **71**, 821 (1979).
[19] M. A. A. Clyne and P. H. Tennyson, J. Chem. Soc. Faraday Trans. 2 **82**, 1315 (1986).
[20] M. A. A. Clyne and J. P. Liddy, J. Chem. Soc. Faraday Trans. 2 **78**, 1127 (1982).
[21] E. H. Fink, H. Kruse, and D. A. Ramsay, J. Mol. Spectrosc. **119**, 377 (1986).
[22] H. Lefebvre-Brion and R. W. Field, *Perturbations in the Spectra of Diatomic Molecules* (Academic, New York, 1986)
[23] B. G. Wicke, R. W. Field, and W. Klemperer, J. Chem. Phys. **56**, 5758 (1972).
[24] E. Hirota, J. M. Brown, J. T. Hougen, T. Shida, and N. Hirota, Pure Appl. Chem. **66**, 571 (1994).
[25] J. Tellinghuisen, Comp. Phys. Commun. **6**, 221 (1973).
[26] R. J. LeRoy, Program Manual for LEVEL, University of Waterloo Chemical Physics Research Report CP-330, 1991.
[27] N. A. Narasimham, V. Sethuraman, and K. V. S. R. Apparao, J. Mol. Spectrosc. **59**, 142 (1976); N. A. Narasimham, K. V. S. R. Apparao, and T. K. Balasubramanian, *ibid.* **59**, 244 (1976).
[28] V. E. Bondybey and J. H. English, J. Chem. Phys. **72**, 3113 (1980).
[29] W. C. Swope, Y. Lee, and H. F. Schaefer, J. Chem. Phys. **70**, 947 (1979).
[30] G. Herzberg *Molecular Spectra and Molecular Structure*, Spectra of Diatomic Molecules, Vol. 1, 2nd ed. (Krieger, New York, 1989).
[31] R. S. Mulliken, J. Chem. Phys. **7**, 14, (1939).
[32] R. S. Mulliken, J. Chem. Phys. **8**, 234 (1940).
[33] H. F. Schaefer III and W. H. Miller, J. Chem. Phys. **55**, 4107 (1971).
[34] MOLPRO is a package of *ab initio* programs written by H.-J. Werner and P. J. Knowles, with contributions from J. Almlöf, R. D. Amos, M. J. O. Deegan, S. T. Elbert, C. Hampel, W. Meyer, K. Peterson, R. Pitzer, A. J. Stone, and P. R. Taylor; P. J. Knowles and H.-J. Werner, Theo. Chim. Acta **84**, 95 (1992).